Mon. Not. R. astr. Soc. (1989) **241**, 325–345

Cosmological deductions from the alignment of local gravity and motion

D. Lynden-Bell, O. Lahav and D. Burstein†

Institute of Astronomy, The Observatories, Cambridge CB3 0HA
†*Physics Department, Arizona State University, Tempe, AZ 85281, USA*

Accepted 1989 April 28. Received 1989 April 26; in original form 1988 December 13

Summary. The precise alignment of the Local Group's motion through the Cosmic Microwave Background and the net optical flux determined from galaxy catalogs is emphasized. Using Peebles' formula, the ratio of the optical dipole to the rate of increase of the optical monopole is used to determine Ω directly on the scale of 1 per cent of the Hubble radius. Allowance is made for unobserved galaxies in all major galaxy associations out to at least 10 000 km s^{-1}. We use Huchra's catalog of radial velocities (*ZCAT Redshift Catalogue*, 1987, privately circulated) to demonstrate that the sources of the optical flux dipole are nearer than 3500 km s^{-1}. The Centaurus Concentration at ~ 4300 km s^{-1} is not the cause of the Local Group's motion, however it contributes, and the long axis of the light quadrupole points to it.

1 Introduction

The flux of light received from a galaxy falls off inversely as the square of its distance. So does the gravity field due to mass associated with that galaxy. Using an overall average mass-to-light ratio, it is then apparent that the vector sum of all the directed light fluxes from galaxies outside the Local Group should be proportional to the gravity field on the Local Group. If that gravity has caused the Local Group's motion relative to the Cosmic Microwave Background, then that motion should be in the direction from which the net light flux comes.

Huchra (1989) has given a good summary of past attempts, using the *Revised Shapley Ames Catalog* and the *IRAS Infrared Galaxy Catalogs* to find such directional agreement; we shall not review this here but major papers following Gott's original suggestion (see Gunn 1985) are given in Table 1.

In our recent papers, Lahav, Rowan-Robinson & Lynden-Bell (1988), Lynden-Bell & Lahav (1988), we have calibrated the diameter functions of galaxies in both the UGC (northern) and ESO (southern) catalogs from complete velocity surveys and we have used these to determine the 'light' dipole at the Local Group due to all galaxies with angular diameters greater than 1.03 arcmin. Study of the way this 'light' dipole builds up as smaller and smaller galaxies are included led us to conclude that at least half of the local gravity field arises from galaxies with diameters greater than 4 arcmin. Galaxies with such large angular diameters typically have

Table 1. Directions from which the net light flux on the Local Group comes $v_{\odot}=(0, 300, 0)$.

				ℓ	b
1969	Conklin	CMB	flux		
1971	Henry	CMB	flux	270	12
1980	Yahil Sandage Tammann	RSA galaxies	light flux	217	78
1982	Davis Huchra	CfA galaxies	light flux	220	69
1983	Shafer Fabian	X-ray background	flux 746±150 km/s	277	19
1986	Yahil, Walker, Rowan-Robinson	IRAS galaxies	flux-weighted bins	248	40
1986	Meiksin, Davis	"	# weighted	235	44
1987	Lahav	ESO,UGC, MCG gals.	θ^2	227	42
1987	Review: Boldt	X-ray back-ground	flux		
1987	Harmon, Lahav, Meurs	IRAS colours	flux	273	31
1988	Lynden-Bell, Lahav	ESO, UGC	θ^2	261	29
1988	Lahav, Rowan-Robinson, Lynden-Bell	IRAS ESO,UGC	flux bins as above	249	38
1988	Strauss, Davis, Yahil	IRAS	redshift survey	231	48
1988	Plionis	Lick	# weighted	237	10
1986	Review: Lubin, Villela	CMB	flux 600 km/s	268	27
1987	Strukov *et al.*	CMB	flux 592 km/s	269	26
1987	Villumsen Strauss	IRAS	flux	239	36

recessional velocities less than 2000 km s^{-1} – much nearer than the 'Great Attractor model' at 4300 km s^{-1} (Lynden-Bell *et al.* 1988; see Appendix A) which we associated with the Centaurus Concentration and to which we had originally attributed a major part of the motion of the Local Group. That attribution had led two of us (DLB, OL) to identify the Centaurus Concentration as the centre of the 'Great Attractor region', a term invented by Alan Dressler to denote an agglomeration of galaxies at a much more extended region. In Appendix A we attempt to clarify the terminology of the various regions in the overall Hydra-Centaurus direction.

At the Vatican meeting Faber pointed out that:

(1) We had omitted an unknown contribution from yet smaller galaxies.

(2) Our association of a given diameter limit with a given redshift is only a very rough indicator of the distance from which the dipole arises.

(3) Our allowance for galaxies behind the murk of the Milky Way was an underestimate since we had assumed a uniform average sky there, whereas our pictures of the all-sky galaxy

distribution show long swathes of galaxies that disappear in the murk and reappear on the other side of the Milky Way. Clearly it would be better to interpolate such structures across the Milky Way rather than replace it by uniform sky.

This paper demonstrates that allowance for all these effects does not change our basic result: the agreement between the direction of the Local Group's motion and the optical dipole remains better than 10° using several different and more detailed treatments of the catalog data. Indeed we are led to regard the directional agreement to be one of the best between theory and observation in extragalactic astronomy.

Our results confirm that the 'light' dipole at the Local Group arises mainly from galaxies with redshifts less than 3,500 km s^{-1} and that any contribution from the Centaurus Concentration at 4300 km s^{-1} is less than 25 per cent (i.e. <150 km s^{-1}). However, we show that Faber's third point is important in that a simple interpolation over the Milky Way band gives a significant change in the *magnitude* of the dipole.

New features employed here are:

(1) Use of Huchra's radial-velocity catalog to allow good estimates of how the contributions to the dipole vary with redshift.

(2) Use of the diameter functions to allow for uncatalogued galaxies associated with those large enough to be catalogued.

(3) Use of Burstein & Heiles' (1978) absorptions rather than the approximate fit to them of Fisher & Tully.

(4) Interpolation over the $|b|<15°$ band by cloning equal area strips of sky on both sides of it and shifting the clones in latitude into the missing band $|b|<15°$. Pictures of the Mock Sky so produced are shown as Figs 1 and 2. We have performed a similar process for the missing band between UGC and ESO, $-2.5<\delta<-17.5$ but have replaced the large galaxies (>3 arcmin) by the true ones catalogued in MCG.

(5) We verified that the Tully *Nearby Galaxies Catalogue* is a subset of our UGC + ESO + MCG + Huchra compilation.

Improvements (1)–(3) have little effect on the results. Far the most important is the replacement in $|b|<15°$ of our former uniform sky by the Mock Sky with the resultant change in the magnitude of the dipole without much change in direction. However, use of the Mock Sky makes an insignificant change to our conclusions as to the depth from which the dipole arises.

We also show how Ω can be determined from a study of the dipole together with the rate of growth of the monopole as smaller and smaller galaxies are included. Use of the Mock Sky makes it possible to study higher moments of the light distribution over the celestial sphere. In particular, we study the quadrupole and give its eigenvalues and eigenvectors.

Section 2 gives the theory and details the corrections we have made in calculating dipoles etc. Section 3 details the results and demonstrates which corrections are important in practice.

Section 4 discusses these findings in the context of Large Scale Streaming motions and 'Great Attractor' models in which a large-scale density enhancement on one side of the sky is the primary cause of streaming.

2 Theory relating flux dipoles to cosmological parameters

2.1 IDEALIZED THEORY

The surface brightness, σ of the extra-galactic sky due to galaxies outside the Local Group can

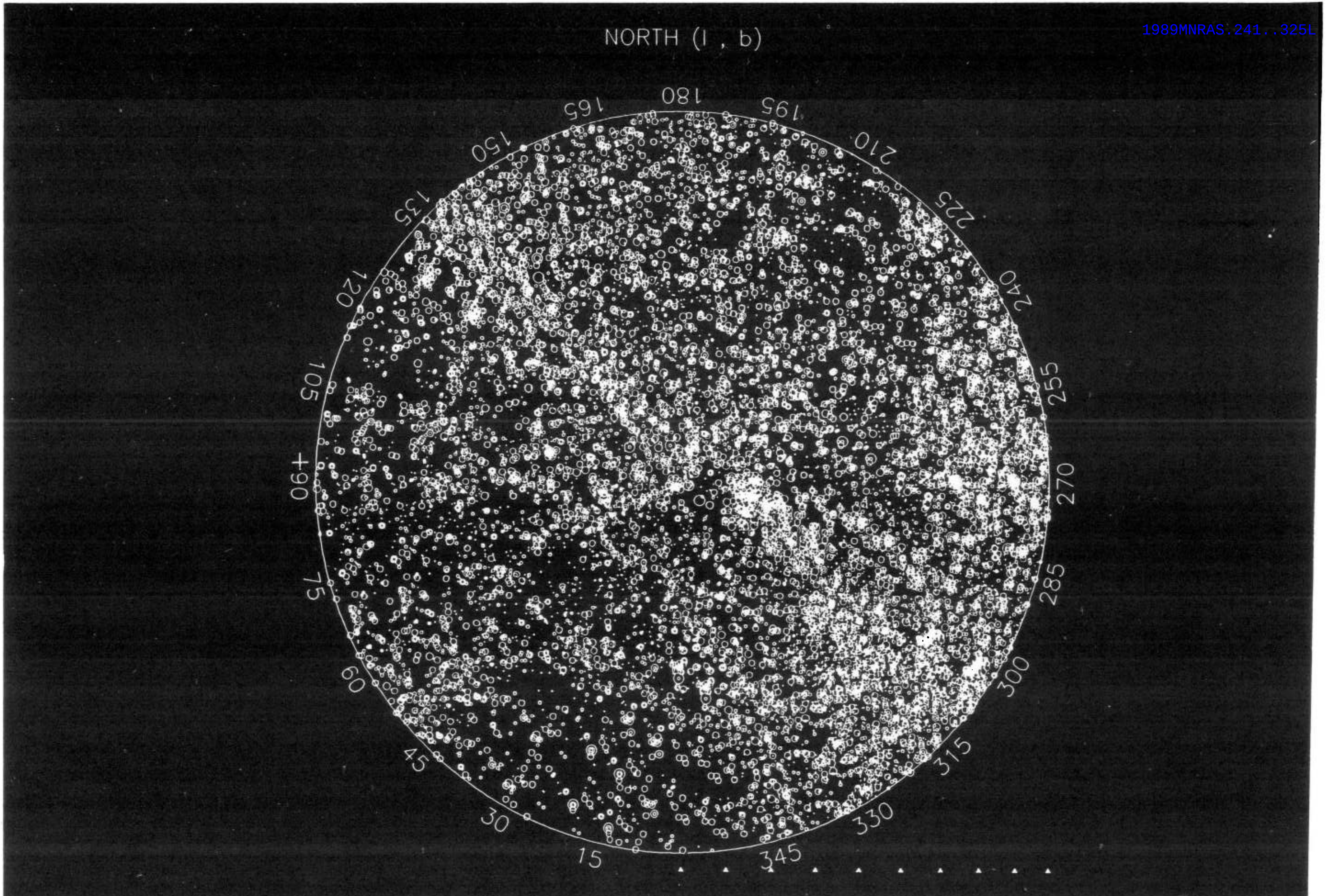

Figure 1. The fully Mocked Sky in which both the $-2.5° > \delta > -17.5°$ strip and the $|b| < 15°$ strip have been filled in by clones of neighbouring strips of sky. The northern galactic hemisphere is shown in an equal area projection. The Local Group's motion is towards $l = 268$, $b = 27$.

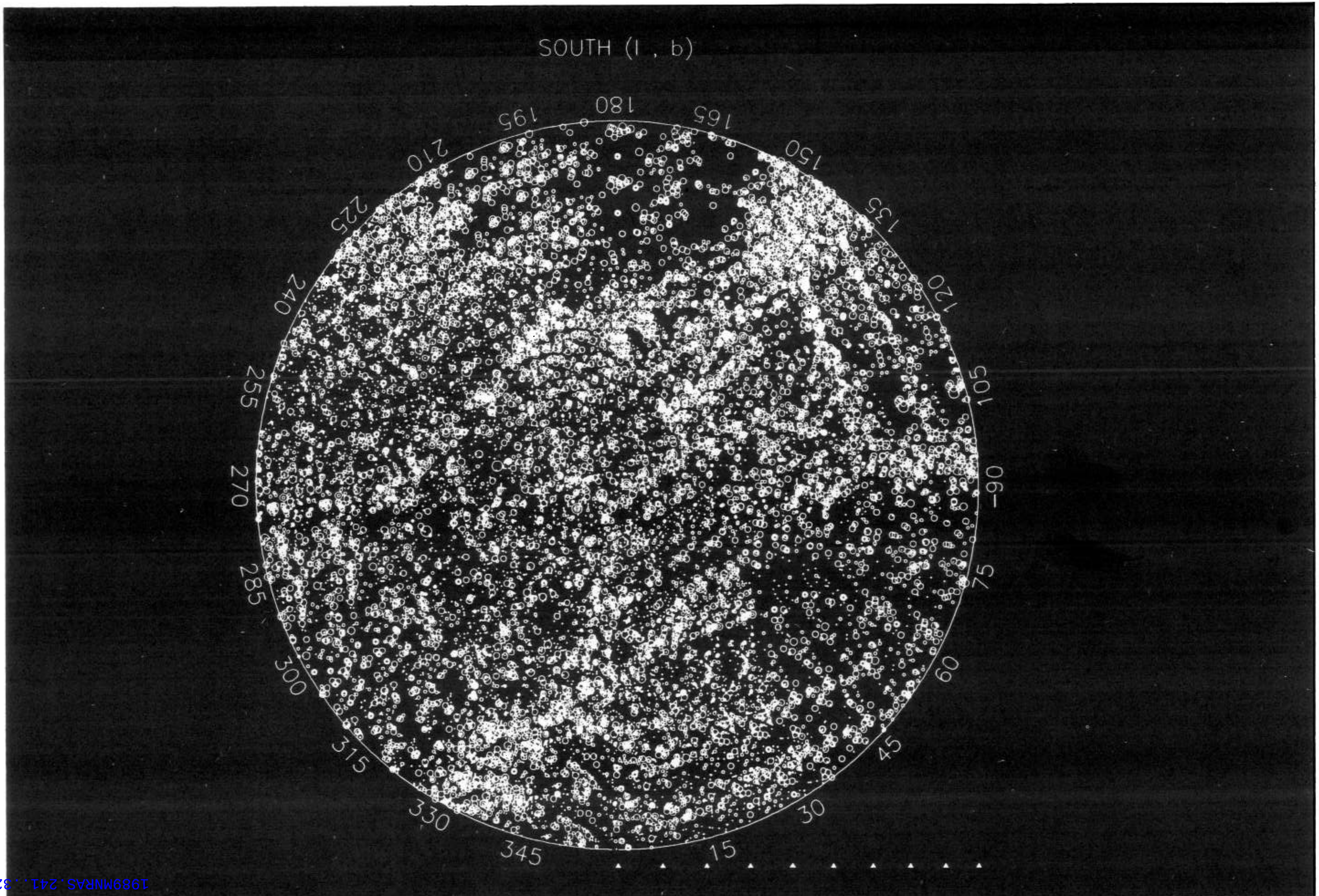

Figure 2. As Fig. 1 but for the southern galactic hemisphere.

be resolved into its monopole, dipole, quadrupole, etc. components by writing

$$\sigma(l,b) = M + \hat{\mathbf{r}}\cdot\mathbf{P} + \hat{\mathbf{r}}\cdot\mathbf{Q}\cdot\hat{\mathbf{r}} + \ldots \qquad (1)$$

where $\hat{\mathbf{r}}$ is the unit vector, $\hat{\mathbf{r}} = (\cos l \cos b, \sin l \cos b, \sin b)$ and the tensor $\mathbf{Q}$ is defined to have zero trace. From the expression it follows that the dipole $\mathbf{P}$ may be re-expressed as a sum over the galaxies that give rise to σ.

$$\mathbf{P} = [3/(4\pi)]\Sigma\hat{\mathbf{r}}L/(4\pi r^2), \qquad (2)$$

where L is the luminosity of a galaxy at distance r in direction $\hat{\mathbf{r}}$ and the sum extends over all galaxies external to the Local Group. With the definition (1), $\mathbf{P}$ agrees with most former works but the factor 3 in (2) was omitted in the Meiksin & Davis' definition.

We shall also be interested in the partial dipoles $\mathbf{P}(<v)$ for which the above sum extends only over galaxies whose recession velocities in the Local Group's frame of rest are less than v. Previously we have, for convenience, studied $\mathbf{P}(>\theta)$ for which the sum extends only over those galaxies whose angular diameters are greater than θ. Analogous to the latter we have the Monopole $M(>\theta)$ defined by

$$M(>\theta) = \frac{1}{4\pi}\sum_{>\theta} L/(4\pi r^2). \qquad (3)$$

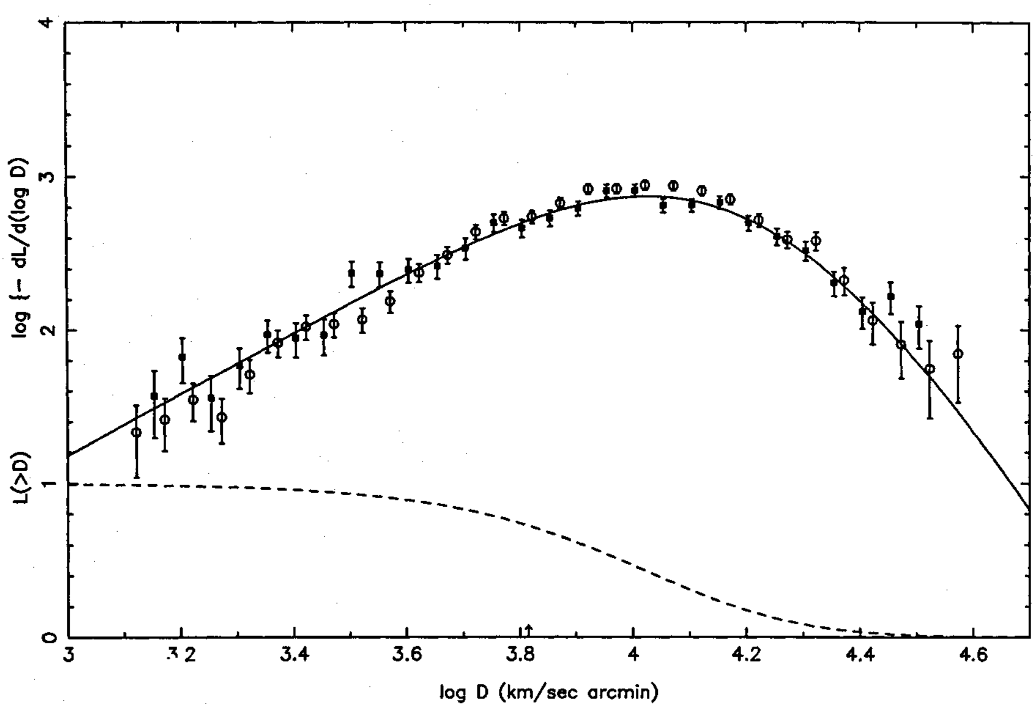

Figure 3. The light function $\mathscr{L}(D)$ plotted at the bottom gives the fraction of all the light of galaxies in a given volume emitted by galaxies of metric diameter greater than D. D is measured in arcmin km s^{-1}, i.e. in units of

$$\left(\frac{1}{60}\frac{\pi}{180}\frac{h_{100}^{-1}}{100}\right)\text{Mpc} = \left(h_{100}^{-1}\frac{\pi}{1080}\right)\text{kpc}.$$

In evaluating $\mathscr{L}$, D^2 has been used to estimate the light as explained in the text. Above is plotted $\log(-d\mathscr{L}/d\log D)$ displaced upwards. The UGC data (open circles) have been shifted by log(1.17) to put them on the ESO diameter scale. The arrow shows the position of D_L (data from Lahav *et al.* 1987).

It is conventional to describe the relative numbers of galaxies at different absolute magnitudes by the luminosity function $\phi(M)$. However, in flux dipoles it is the light from the galaxies rather than their numbers which is of significance. We shall find it convenient to use the major absolute diameters of galaxies D_0 as ordinate and to define the function $\mathscr{L}(D_0)$ to be that fraction of all the light emitted by galaxies in a given volume which is emitted by galaxies with diameters greater than D_0. Thus $\mathscr{L}(0)=1$ and $\mathscr{L}(\infty)=0$ (see Fig. 3). Let $\rho_{\rm L}(\mathbf{r})\,d^3r$ be the total light emission by all galaxies in the volume d^3r about the position $\mathbf{r}$. Then

$$M(>\theta)=\frac{1}{4\pi}\int \mathscr{L}(r\theta)\rho_{\rm L}(\mathbf{r})(4\pi r^2)^{-1}\,d^3r, \tag{4}$$

and

$$\mathbf{P}=\frac{3}{4\pi}\int \hat{\mathbf{r}}\rho_{\rm L}(\mathbf{r})(4\pi r^2)^{-1}\,d^3r. \tag{5}$$

Now at small θ most of the contribution to M comes from large distances where $\rho_{\rm L}(r)$ may be replaced by its average and thus, for small θ, $\theta^2 dM/d\theta$ is approximately constant.

$$-\theta^2\frac{dM}{d\theta}=\frac{\langle\rho_{\rm L}\rangle}{4\pi}\int_0^\infty\left(-d\mathscr{L}/dD_0\right)D_0\,dD_0=\frac{\langle\rho_{\rm L}\rangle}{4\pi}\bar{D}_0=\text{constant}, \tag{6}$$

where $\bar{D}_0$ stands for the definite integral and $\langle\rho_{\rm L}\rangle$ is the mean luminosity density.

If we now define $\Delta(\mathbf{r})=[\rho_{\rm L}(r)/\langle\rho_{\rm L}\rangle]-1$ then, since the uniform sky gives no dipole

$$\mathbf{P}/|\theta^2\,dM/d\theta|=3\bar{D}_0^{-1}\int \hat{\mathbf{r}}\Delta\cdot(4\pi r^2)^{-1}\,d^3r. \tag{7}$$

The integral on the right-hand side is closely related to the gravity field of external galaxies at the Local Group. For assuming excess light and excess mass are proportional $\Delta=b\delta\rho/\rho_0$ where b is the 'bias' parameter (Kaiser & Lahav 1988).

$$\mathbf{g}=(4\pi G\rho_0/b)\int \hat{\mathbf{r}}\Delta\cdot(4\pi r^2)^{-1}d^3r. \tag{8}$$

Furthermore, by Peebles' (1980) formula for linear perturbations in the expanding universe, we have

$$\mathbf{v}=(\tfrac{2}{3})\Omega^{-0.4}\mathbf{g}/H, \tag{9}$$

where $\mathbf{v}$ is the peculiar velocity induced by the perturbation, H is Hubble's constant and Ω is the density parameter of the universe ρ_0/ρ_c. Combining equations (7)–(9), we find

$$\mathbf{P}/|\theta^2 dM/d\theta|=\kappa b\Omega^{-0.6}\mathbf{v}, \tag{10}$$

where

$$\kappa=3H\Omega/(\bar{D}_0 8\pi G\rho_0/3)=3/(H\bar{D}_0). \tag{11}$$

Now, although evaluation of $\bar{D}_0$ requires us to know true distances to galaxies, the evaluation of $H\bar{D}_0$ from a complete redshift survey only requires their redshifts in the Hubble flow. In fact we evaluate the function $\mathscr{L}$ not as a function of true diameter D_0 but as a function of $D=v\theta$, where θ is the angular diameter. Since $D = HD_0$, the product $H\bar{D}_0$ can be rewritten from equation (6) as

$$\bar{D} = H\bar{D}_0 = \int_0^\infty -(D\, d\mathscr{L}/dD)\, dD. \tag{12}$$

With this evaluation, equation (10) becomes an equation for $b\Omega^{-0.6}$ in terms of the dipole and monopole moments of the extragalactic 'light'.

Both expression (7) and (8) are derived from Newtonian physics. Obviously there is room here for K-corrections, cosmological corrections, etc. but with the dipole arising from rather close by, these will not make significant changes. Formula 2–8 relating the gravity field to Δ must require changes too, because contributions to the gravity dipole from high redshift objects will come in diluted. A full gauge invariant discussion of what should replace 2–10 for dipoles arising on a cosmological scale is called for, but is not important for our rather local problem.

2.2 PRACTICAL EVALUATION PROBLEMS

The ESO catalog does not give magnitudes. it gives major and minor diameters and claims completeness down to major diameters of 1 arcmin. The UGC catalog also gives diameters, but measured off different plates that go to a different depth. There is no reason to assume that a galaxy with major diameter of say 2 arcmin on the ESO system is the same angular size as one of 2 arcmin on the UGC system. There is some system in the surface brightnesses of galaxies, so it is not surprising that the squares of the diameters of galaxies are well correlated with luminosity. There are, of course, well known low surface brightness galaxies, but these do not contribute significantly to the total light nor are they well represented in the galaxy catalogs. For simplicity of explanation we have given the general theory in terms of light flux. In our practical evaluations we shall not use the unmeasured light flux from each galaxy, but replace it by the square of the galaxy's major angular diameter.

Going back through the general theory we find that use of θ^2 automatically gives the correct inverse square distance weighting. Thus, provided that galaxies at a given distance have D_0^2 correlated with mass, the sum of the $\theta^2\hat{\mathbf{r}}$ will be as good as the sum of the fluxes. We are not primarily interested in the masses of the galaxies themselves, but rather the total masses with which they are associated. This will mainly be in some unknown dark form, so there is no guarantee that total light flux would be a better measure of it than the sum of the squares of the galaxy diameters. We use major diameters following the result of Burstein & Lebofsky (1986) that major diameters of spiral galaxies are statistically independent of inclination to the line of sight. In this respect they have a real advantage over light fluxes, since the latter are dependent on the inclination at which the galaxy is seen. Analogous to equation (2), the dipole we try to evaluate is actually

$$\mathbf{P} = (3/4\pi)\Sigma\hat{\mathbf{r}}\theta_c^2 \tag{13}$$

where θ_c is the square of the major angular diameter corrected for absorption and the sum in principle extends over all galaxies outside the Local Group.

Four major problems are encountered in evaluating $\mathbf{P}$:

(a) The differences between the galaxy catalogs.

(b) Compensation for galaxies too small to have been cataloged but sufficiently numerous and so distributed as to give a significant dipole contribution.

(c) The Milky Way region, $|b| \leq 15°$, where absorption is so strong and confusion so acute that galaxy counts mean little. We may add to this the $-2.5° \geq \delta \geq -17.5°$ strip between UGC and ESO.

(d) Galactic absorption in the $|b| \geq 15°$ zone.

We treat these in turn:

(a) The CfA redshift surveys are complete to a known cut-off in a known region of the sky. So is the Southern redshift survey. Using this completeness Lahav has deduced the diameter functions $\phi(v\theta)$ that describe the numbers of galaxies per unit volume of redshift space which have diameters D in each decade of $v\theta$. This is done separately for unobscured regions of both the Northern UGC and the Southern ESO galactic caps. From these functions we can deduce the modified light function $\mathscr{L}(D)$ which gives the fraction of the total ΣD^2 per unit volume that comes from galaxies of 'diameters' greater than D. Thus

$$\mathscr{L}(D) = \int_D^\infty D^2 \phi(D)\, dD \Big/ \int_0^\infty D^2 \phi(D)\, dD. \tag{14}$$

$\mathscr{L}$ does not depend on the normalization of ϕ. Notice that $D = v\theta$, where v is the velocity in the Hubble flow. Thus $\mathscr{L}$ is defined not as a function of the true diameters but as a function of the angular diameter times the Hubble constant. It is that combination which is both needed and more directly observed. We get two different $\mathscr{L}(D)$ functions from the different surveys each of which is in an area covered by one of the two catalogs. Both $\mathscr{L}(D)$ functions may be fitted with the mathematical form

$$\mathscr{L}(D) = (1 + t/2)/(1 + t/\beta)^{\beta - 1} \tag{15}$$

with $t = (D/D_L)^2$ and $\beta = 5$ (see Fig. 3).

For ESO we find that the characteristic diameter is

$$D_L = 6538 \pm 284 \text{ arcmin km s}^{-1}$$

while for UGC the corresponding diameter is

$$D_{LU} = 5588 \pm 243 \text{ arcmin km s}^{-1}.$$

We deduce that the measurements of diameters of galaxies on the somewhat deeper ESO plates are on average $D_L/D_{LU} = 1.17 \pm 0.07$ times larger than the measurements on the less deep Palomar plates used in the North. This ratio agrees well with our former estimates 1.13 ± 0.05 from diameter function fitting (and 1.11 from fitting the relative numbers of galaxies in the small diameter bins which show the growth of numbers expected from a uniform universe). Since we shall be centering our work around the $\mathscr{L}$ function, we adopt the value 1.17 for the scaling. Hereafter all UGC diameters are multiplied by this number to put them on the same scale as ESO diameters. On this basis we proceed as though the two catalogs were otherwise identical.

This procedure itself may be corrupted by streaming. Lahav used velocities corrected to the frame of the Local Group (and for Virgocentric infall) to evaluate D_L and D_{LU} since that is the best frame near here. Had he used velocities relative to the CMB and assumed (probably wrongly) that the galaxies were expanding uniformly in that frame, then D_L would be decreased and D_{LU} increased both by about 300 arcmin km s^{-1} (i.e. 5 per cent).

We may now evaluate κ of equations (11) and (12).

$$\bar{D} = \int_0^\infty -D\, d\mathscr{L}/dD\, dD = D_L 3\pi 5^{3/2}/64 = 1.65 D_L, \tag{16}$$

where the integral is evaluated in Appendix II. Hence from equation (11)

$$\kappa = 3/\bar{D} = 1.82/D_L. \quad (17)$$

(b) Major galaxy concentrations have more than $\frac{1}{3}$ of their light provided by galaxies with diameters greater than $1.8D_L \simeq 11\,700$ arcmin km s^{-1}, so in a catalog complete to 1.17 arcmin, all major galaxy concentrations out to Hubble velocities of 10 000 km s^{-1} will be represented. Our problem is that the distant ones are under-represented because the diameter limit will have cut away contributions from all but the largest galaxies. Provided the observed galaxies have redshifts it is relatively easy to use our knowledge of the $\mathscr{L}$ function to allow for the unobserved galaxies associated with them. At Hubble velocity v the fraction of the total light that will be observed above the diameter limit of the catalog θ_{mc} will be $\mathscr{L}(v\theta_{mc})$. Thus, if each observed galaxy is given a weight $1/\mathscr{L}(v\theta_{mc})$, the galaxies associated with the observed ones will be properly accounted for, even if they are too small to have been counted individually. There will be galaxies too far away to be included at all, but the belief that the Universe is homogeneous in the large, leads one to believe that little of the dipole can arise from beyond 10 000 km s^{-1}. Furthermore, we may check this by finding out how the dipole grows as the limit is changed. For each galaxy, 'G', with angular diameter $\theta(\geq \theta_m)$ which has no measured v, we must estimate $\langle 1/\mathscr{L}(v\theta_c)\rangle$ statistically. This we do by averaging $1/\mathscr{L}(v\theta_c)$ for all galaxies with θ_{mc} fixed at the absorption-corrected catalog-limit in the direction of the galaxy G. We average $1/\mathscr{L}$ using the velocities v of all those galaxies in Huchra's catalog that have the same true angular diameter θ_c as galaxy G. Since the radial velocities are unbiased at given θ, this should give a good statistical estimate.

In practice the $1/\mathscr{L}$ functions are only exceptionally greater than 10 and $\langle 1/\mathscr{L}\rangle$ is between 1 and 2.3 for every θ bin. It is no real surprise to find that leaving out the $1/\mathscr{L}$ factors only changes the dipole a little. However, inclusion of these factors adds considerably to our confidence that galaxies smaller than the catalog limits and within 10 000 km s^{-1}, are unlikely to change our result.

(c) To interpolate the galaxies counted elsewhere over the poorly counted strip $-2.5 \geq \delta \geq -17.5$, or the galactic zone of avoidance $|b| < 15$ we adopt a crude but effective cloning procedure. An equal area projection of the sky is obtained by using right ascension α and $\sin\delta$ as orthogonal coordinates. In this projection the poorly counted strip is horizontal. On each side of it we cut horizontal slots, each equal to half its thickness. Within each slot we clone the galaxies together with their diameters and absorptions and then move the clones in $\sin\delta$ to replace the poorly counted strip completely. Where the original cloned regions were in the $|b| < 15$ zone of avoidance, those regions are replaced by the regions with $|b| > 15$ that would have been moved into the $|b| < 15$ zone. Those good at jigsaw puzzles will realize that the pieces fit. In this way all the $-2.5 > \delta > -17.5$ strip outside $|b| < 15$ is replaced by clones from neighbouring latitudes. We then rotate coordinates to galactic ones and repeat the process for $|b| < 15$ with $\sin b$ replacing $\sin\delta$ and l replacing α. In the whole process about 35 per cent of the sky has been cloned. Having completed the above procedure we decided it was more sensible to use the *bright* galaxies counted by Vorontsov-Velyaminov & Archipova rather than the bright clones there. Thus we deleted all mock galaxies with diameters greater than 3 arcmin in the $-2.5 > \delta > -17.5$ strip which had $|b| > 15$ and inserted the large galaxies of the MCG found in that region. To put them on the same diameter system as ESO, we used the conversion formulae of Fouqué & Paturel (1985) and then cut at 3 arcmin diameter.

We believe the above interpolation procedure is probably more realistic than replacing unobserved regions with the mean of the rest of the sky. However, our procedure produces correlated fluctuations, so although it correctly interpolates the obvious streaks of galaxies, it may overestimate the net dipole. We therefore compare the dipole deduced from the Mock

Sky with that obtained from our former Average-Sky procedure. The Mock Sky has a major effect on the magnitude of the dipole but causes no marked change in the dipole's direction.

(d) Galactic absorption – since Burstein has shown that a galaxy's major diameter is statistically independent of the inclination at which the galaxy is seen, we do not correct for its internal absorption. We concern ourselves with extinction by the Milky Way which lessens the measured diameters. Thus galaxies above the catalog limits have angular diameters smaller than their true ones and some galaxies, that would have appeared just larger than the catalog's diameter limit, now appear so small that they are not included. We must correct for both these effects.

We use Burstein & Heiles' (1978) extinctions (replacing the negative ones by zero as they prescribe) and since θ^2 behaves like apparent luminosity, we correct them to θ_c using the formula

$$\theta_c = \theta 10^{A_B/5}.$$

In the regions where Burstein & Heiles do not give A_B, we use the interpolation formula of Fisher & Tully (1987). To allow for galaxies that are really above the catalog's angular diameter limit which have been sent below it by absorption, we use the cumulative number function and the cumulative θ^2 function observed in the galactic polar caps. We call those functions $N(>\theta)$ and $K(>\theta)$, where

$$K = \int_0^\infty \theta^2(-dN/d\theta)/\mathscr{L}(\theta_m v)\, d\theta.$$

θ_m denotes the catalog's angular diameter limit at zero absorption and its larger absorption corrected limit is θ_{mc}. In evaluating $K(\theta)$ over the polar caps, v is the velocity of the galaxy being included in the sum but if its velocity is unknown, $1/\mathscr{L}$ is replaced by $\langle 1/\mathscr{L} \rangle$. At the pole the mean contribution to $\Sigma\theta^2/\mathscr{L}$ of galaxies with diameter between θ_m and θ_1, per galaxy observed with diameter $>\theta_1$ is

$$[K(\theta_m) - K(\theta_1)]/N(\theta_1) = F(\theta_1, \theta_m).$$

To the contribution $\theta_c^2/\mathscr{L}(v\theta_{mc})$ that we have from each galaxy in an absorbed region, we add $F(\theta_{mc}, \theta_m)$ to compensate for the missing galaxies with true diameters between θ_m and θ_{mc}. Again wherever velocities are not known we use the average value of $1/\mathscr{L}$ averaged over galaxies of the same corrected diameters which have known velocities.

Our formula for the total dipole is thus

$$\mathbf{P} = \frac{3}{4\pi} \sum_{\theta > \theta_m} \hat{\mathbf{r}}(\theta_c^2/\mathscr{L} + F),$$

where the sum extends over all galaxies with raw-measured diameters $>\theta_m$ in both the real and the cloned parts of the Mock Sky. $1/\mathscr{L}$ stands for $1/\mathscr{L}(v\theta_m)$, where v is known, and otherwise $\langle 1/\mathscr{L}(v\theta_m)\rangle$ averaged over objects of the same θ_c but with known v. In analysing $\mathbf{P}$, it is interesting to discover which regions of the sky it comes from and at what depth. For this we need $\mathbf{P}(<V)$ as a function of the Hubble velocity V. To find $\mathbf{P}(<V)$ we proceed as before, but where a galaxy has a measured velocity v, we only include it in the sum if $v<V$. When the galaxy in question has no measured velocity, we ask what fraction of these galaxies at the same θ_c, whose velocities have been measured, have $v<V$, and include only that fraction $f(<V, \theta_c)$, in the sum. Similarly, only the fraction $\int_{\theta_m}^{\theta_{mc}}[dF(\theta, \theta_m)/d\theta]f(<V, \theta)\, d\theta$ of $F(\theta_{mc}, \theta_m)$ will contribute in the $v<V$ range, so our final expression for the part of the dipole that comes from

galaxies with velocities $< V$ is

$$P(<V)=\frac{3}{4\pi}\sum_{\theta\geq\theta_m}\hat{\mathbf{r}}\left(\theta_c^2 f/\mathscr{L}+\int_{\theta_m}^{\theta_{mc}} dF(\theta,\theta_m)/d\theta\, f(<V,\theta)\, d\theta\right)$$

with the same understanding as before on how $1/\mathscr{L}$ is evaluated.

The monopole is easier to evaluate, as it is defined as a function of θ and only down to θ_m. Thus no $1/\mathscr{L}$ factors are needed. K is replaced by K_1, the function obtained by omitting the $1/\mathscr{L}$ factor and the resulting F we call $F_1(\theta_1, \theta_m)=[K_1(\theta_m)-K_1(\theta_1)]/N(\theta_1)$

$$M(>\theta)=(4\pi)^{-1}\sum_{\theta_c>\theta}[\theta_c^2+F_1(\theta_{mc},\theta_m)]$$

the sum extends over all galaxies with $\theta_c > \theta$ and θ_{mc} is the absorption corrected catalog limit evaluated with the absorption of the galaxy being counted.

For completeness, we define the corresponding dipole

$$P_1(>\theta)=(3/4\pi)\sum_{\theta_c>\theta}\hat{\mathbf{r}}[\theta_c^2+F_1].$$

This is the quantity we evaluated in our earlier papers (Lahav *et al.* 1988, Lynden-Bell & Lahav 1988).

3 Results

Fig. 4 shows the growth of the x, y, z ($\cos l \cos b$, $\sin l \cos b$, $\sin b$) galactic components of the dipole where the total dipole is normalized to 1. Concentrating first on the full line, we see that most of the contribution comes from the $-y$ direction $l=270$, $b=0$ although there is some positive z contribution. The x-component towards the Galactic Centre is always small. 80 per cent of the amplitude of the final dipole is attained from galaxies with $v<4000$ km s^{-1}, while over half comes from galaxies with $v<2000$ km s^{-1}. These estimates are in good agreement with those given in our Vatican paper based on $P(>\theta)$. The z-component is almost all present by 2000 km s^{-1} beyond which it remains almost constant. Much of this component is due to the Virgo and Ursa Major clusters which are both at the same distance and close to the galactic pole. Notice that the $-y$ component at 1000 km s^{-1} is almost as large as the z component and at 2000 km s^{-1} the $-y$ component is already larger. This demonstrates that even at these low velocities the Centaurus region is already contributing strongly and Virgo-Ursa Major is not dominant. Along with the full lines in Fig. 4 are two others that follow it closely and a dotted line that shows a significant deviation in the z-component. The dashed line is a test of the efficacy of our averaging of $1/\mathscr{L}$. In place of the true values of $1/\mathscr{L}$, formerly used for galaxies that have measured velocities, we have used the average $\langle 1/\mathscr{L}\rangle$, which is a function of θ, for *all* galaxies. Clearly this procedure makes no difference to the result. Of more significance are the dot-dashed curves that can barely be distinguished from the other two. Here every galaxy has been treated as though its velocity had not been measured. The only residual use of the velocities being to evaluate statistically the average values of $\langle 1/\mathscr{L}\rangle$ as a function of θ and the function $f(v, \theta)$ which gives the probability that a galaxy of angular diameter θ in our sample has velocity v. Thus the dot-dashed curve is deduced from angular diameters and is an estimate of the dipole as a function of distance (not velocity) with the distances (translated into velocity units) by use of the mean relations determined from the whole sky. An overall

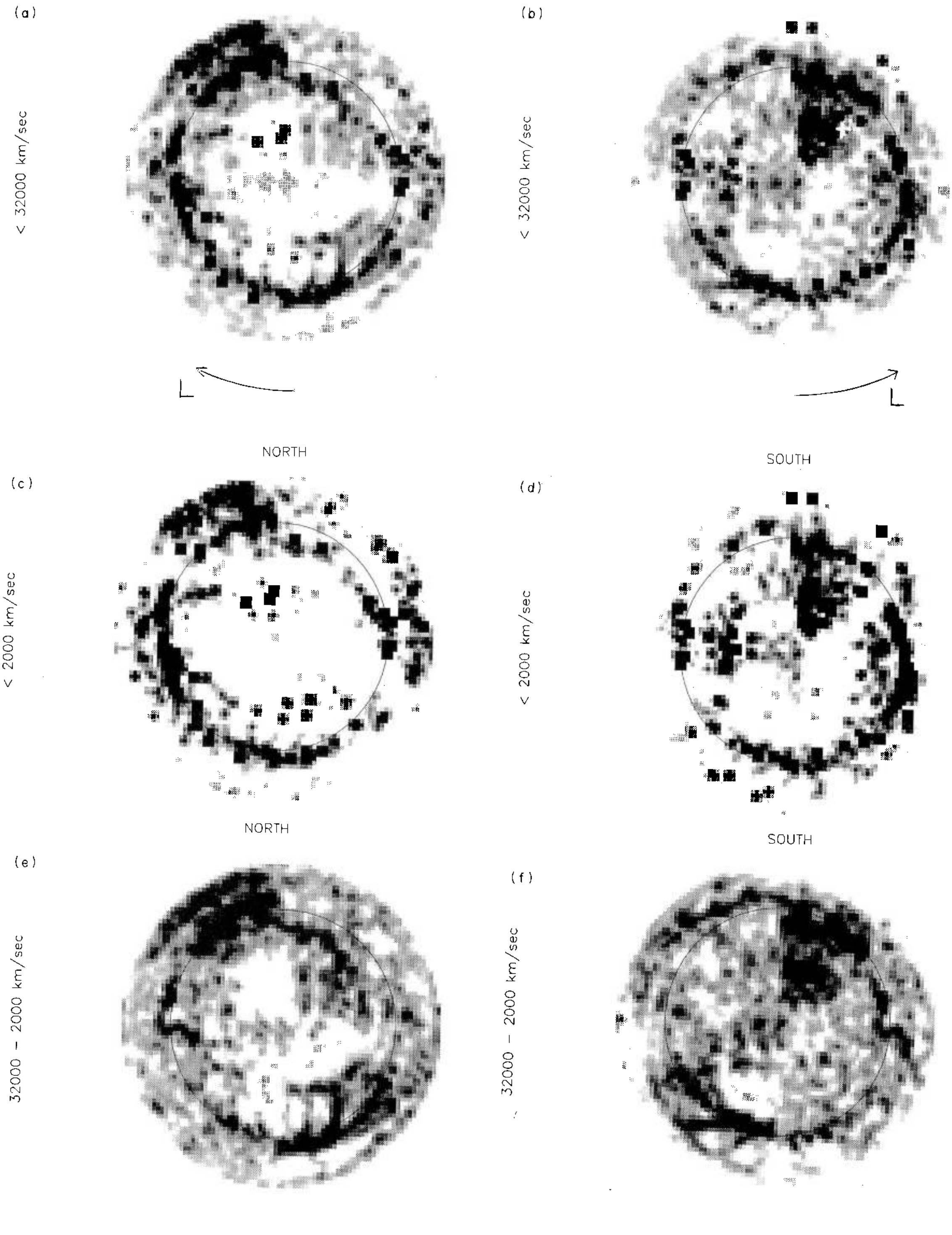

Plate 1. Supergalactic projections of the surface brightness of the extragalactic Mock Sky arising from galaxies in different velocity ranges. Each projection shows the whole sky in an equal area projection with one supergalactic pole at the centre and the other at the outer circumference. The supergalactic plane is the circle drawn. Because the hemisphere outside the circle is severely distorted by the projection, each diagram is accompanied by another centred on the opposite pole. The grey-scales are chosen so that black is more than twice the mean surface-'brightness' and white is less than a half of that mean. North-centred pictures have supergalactic longitude, L, measured clockwise from the bottom. In south-centred pictures L is anticlockwise to preserve the orientations of the real sky. (a) Centred on the northern supergalactic pole showing the 'brightness' as corrected to allow for all light emitted by galaxies up to at least 10000 km s^{-1}. (b) As (a), but centred on the southern supergalactic pole. The white cross indicates the direction of the local group's motion. (c)–(d) As (a) and (b), but showing only the 'brightness' that arises from galaxies with $v < 2000$ km s^{-1}. (e)–(f) The 'brightness' arising from the galaxies with $v \geq 2000$ km s^{-1} and contained in (a) and (b).

[facing page 336]

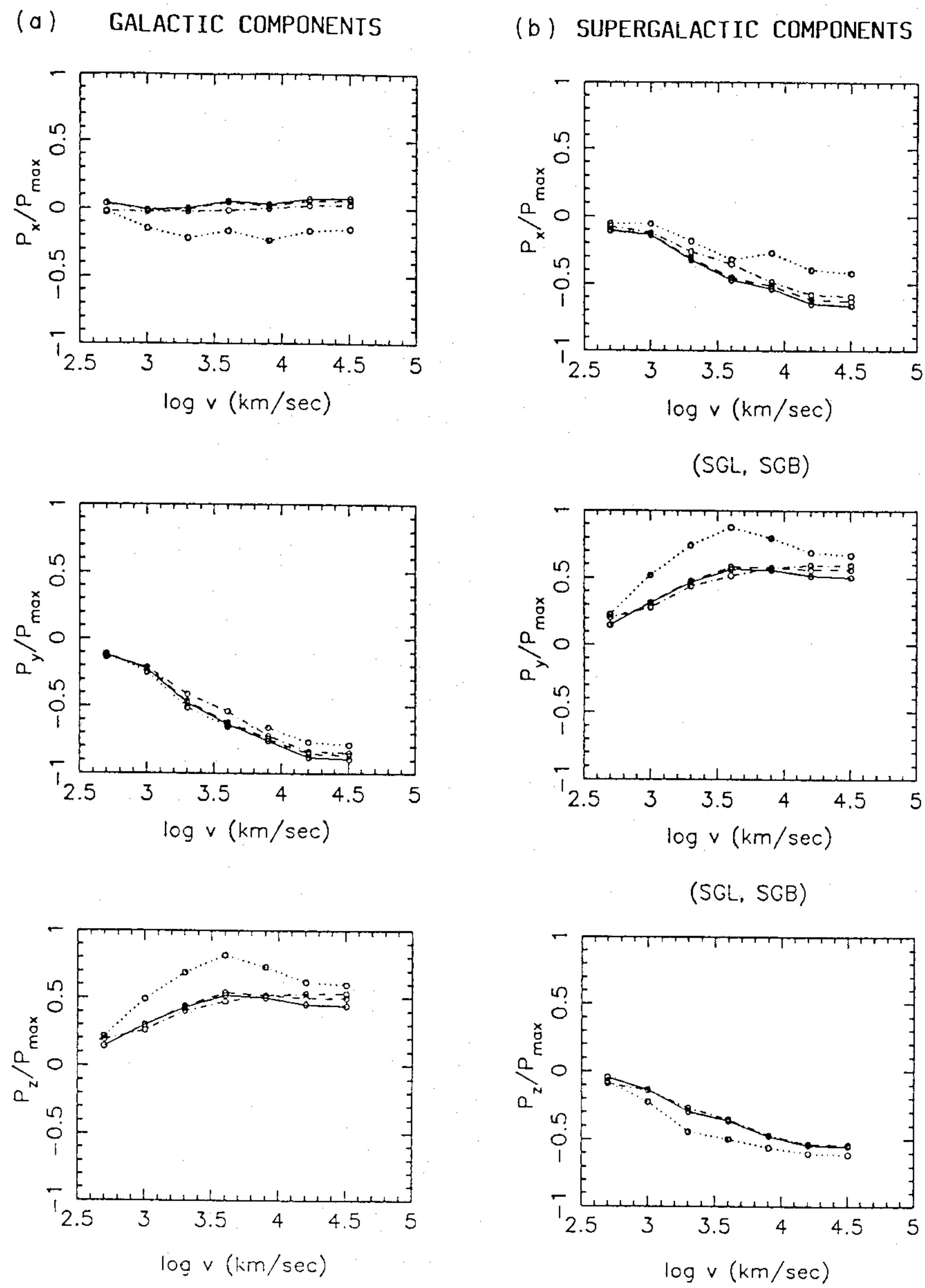

Figure 4. The growth of the galactic components of the dipole as the depth of the sample is increased. Full line, Mock Sky with velocities used when available; dotted line, the same but with average value of $1/\mathscr{L}$ used for all galaxies; dash-dotted line, the same but with velocities ignored even for binning. They are restored only statistically from the fraction of these galaxies at angular diameter θ with measured velocities that have velocity less than v; dashed line as full line but with Average Sky replacing Mock Sky in both poorly counted strips of sky. (b) Translates the dipole into its supergalactic components.

streaming motion might upset partial dipoles $P(<V)$ because the cut-off would be deeper in the direction opposed to the stream and less deep in the direction along the stream. The fact that the full and dot-dashed curves almost coincide, shows that this effect contributes negligibly to our partial dipoles. Huchra's catalog has velocities for all the galaxies with

diameters greater than 6 arcmin and is more than 50 per cent complete at 2 arcmin. For galaxies between 1 and 2 arcmin it is 25 per cent complete.

We now turn to the more discrepant dotted lines. These have been determined without the cloning procedure used to obtain the Mock Sky but rather by replacing both the $-2.5>\delta>-17.5$ and the $|b|<15$ zones by the average 'surface brightness' per unit solid angle found from the rest of the sky. For the dipole this procedure gives a zero contribution for $|b|<15$, since that is symmetrically placed but some contribution comes from the rest of the MCG strip. Details of this our former procedure are given in Lahav *et al.* (1988).

Fig. 4(b) shows the supergalactic components of the dipole. Interestingly the component out of the supergalactic planes grows continuously out to beyond 5000 km s^{-1}.

Fig. 5 shows the direction of the partial dipoles on the sky. The points are labelled P.5, 1, 2, 4, ∞ corresponding to **P**(<500), **P**(<1000), **P**(<2000), **P**(<4000) and the total value of *P*. The circled symbol ∞ shows **P**(∞) calculated with the average sky instead of the Mock Sky. Whichever procedure is used, the direction of the full dipole is remarkably close to the Local Group's motion relative to the Cosmic Microwave Background, '+'. When we compare the magnitudes of the dipoles, we see that the Mock Sky treatment is giving a significantly different total from the 'average sky' treatment of the missing strips. With such a large difference between these estimates of the total dipole, our lack of information from behind the Milky Way will prevent an accurate determination of Ω from the magnitude of the total dipole. However, we need not await a complete 21-cm mapping of galaxies behind the Milky Way. The contributions to the *z*-component of the dipole all contain the factor sin *b* which is zero on the galactic plane and small in the $|b|<15$ strip, whose two sides tend to cancel. Thus we can try to evaluate Ω off the *z*-component of equation (10) which will be insensitive to galaxies close to the galactic plane. Our two estimates of P_z using Mock Sky and Average Sky are indeed closer than the two estimates of |**P**|. Furthermore, the estimates of $\theta^2 dM/d\theta$ from the different procedures help to correct the discrepancy.

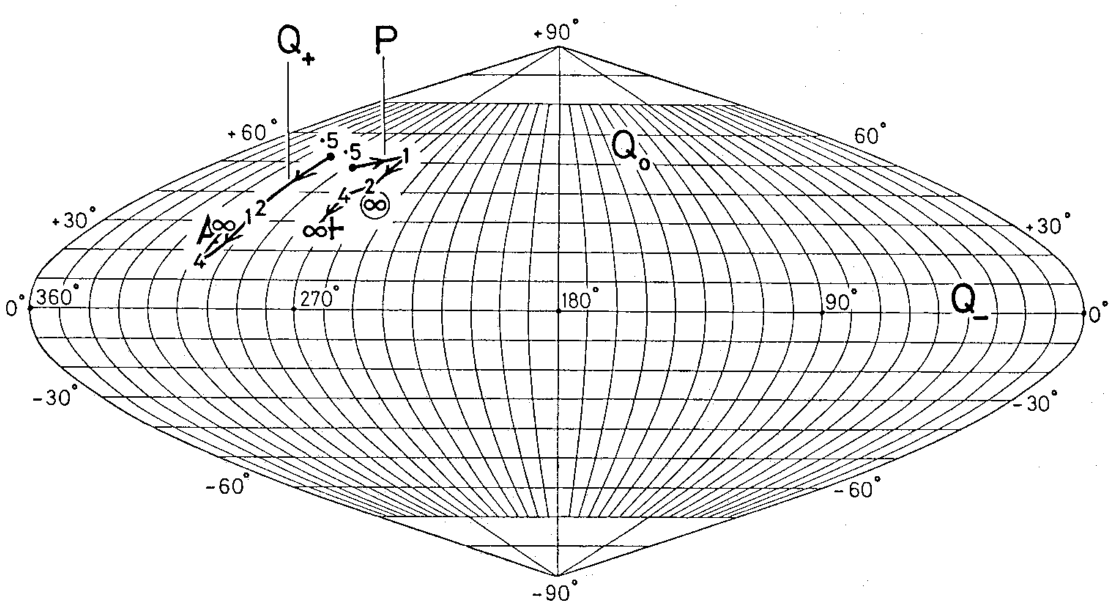

Figure 5. The directions of the dipole and the quadrupole eigenvectors as a function of depth. 0.5, 1, 2, 4 refer to the upper velocity limit in thousands of km s^{-1}. + is the direction of the Local Group's motion. 'A' is the direction of the Centaurus Concentration identified as the Great Attractor. Q_+ is the eigenvector of the quadrupole that is largest for large *V*. Q_- is the quadrupole eigenvector toward the supergalactic poles. Q_0 is the third axis of the quadrupole which is actually the largest for $v<1000$ km s^{-1} where it is drawn in the Ursa Major cloud of the supergalactic plane.

The only outstanding source of difficulty is the $-2.5 \geq \delta \geq -17.5$ strip on which we have only the MCG data. The main z-dipole contributions come from galaxies that are quite large, most of it from galaxies ≥ 3 arcmin, for which MCG is probably pretty complete. It is for this reason that we use the large galaxies from MCG and only use the Mock Sky for the galactic plane and for the small galaxies <3 arcmin in the $-2.5 \geq \delta \geq 17.5$, $|b| > 15$ part of the MCG strip. This should give us the best z-component of dipole attainable at present. Some improvement can be expected as soon as Corwin has re-counted and re-measured the galaxies with $\theta > 1.9$ arcmin in the MCG strip, with some overlap to both ESO and UGC which should prove most important for calibration.

Table 2 gives both the total dipoles and the values of $\theta^2 dM/d\theta$ determined from both the Mock Sky and the Average Sky procedures. Averaging the Mock Sky and Average Sky results together gives concordant results of 0.37 for $\Omega^{0.6}/b$. It is quite possible that b is as large as 2.7, so this result supports the idea that Ω could be 1. If we took b to be 1, then Ω would be 0.19. However, the errors on this determination are quite large. We can only determine $\log(\theta^2 dM/d\theta)$ to an accuracy of 0.1 and the discrepancies between different estimates of $|P|$ are 0.3 in the log. From these we estimate that our estimates of Ω are likely to have errors of at least a factor 2 even before taking uncertainties in b into account.

4 Light quadrupoles and local gravity

Unlike the cosmic microwave background, the light from galaxies has significant quadrupole moments. Fig. 6 plots the magnitude of the dipole and monopole moments from galaxies with velocities $<v$ as a function of v. It also plots Q_+, the eigenvalue of the quadrupole which is most positive at large v. There is obvious evidence of incompleteness in the saturation of M (and Q_+) above 10000 km s^{-1}. As explained above, we cannot hope to be complete in those regions. We also plot Q_0, the eigenvalue that is closest to zero for large v. The third eigenvalue Q_- is negative and is, apart from sign, the sum of the other two. The direction of this negative eigenvalue Q_- is remarkably constant and close to the supergalactic poles. For the Mock Sky the (l, b) direction of Q_- for galaxies with $v < 500$ is (42,5), while for large v this changes to (41,6). For comparison, the supergalactic pole lies at (47,6). It could be argued that the eigenvector of Q_- should define the supergalactic pole, but it is wiser to trust de Vaucouleurs' perusal of the real sky rather than a mathematical prescription applied to a mock sky. His prescription certainly follows well the supergalactic band in the Northern sky, although the Pavo-Indus-Telescopium band of galaxies in the South deviates from his standard supergalactic equator.

Table 2.

	Mock Sky	Average Sky	Means
$\|P\|$	8486	4288	
P_z	3739	2560	
$\log_{10}(\theta^2 dM/d\theta)$	4.2	4.1	
$\Omega^{0.6}/b$	0.312	0.490	.401
ditto based on P_z	0.320	0.374	.347

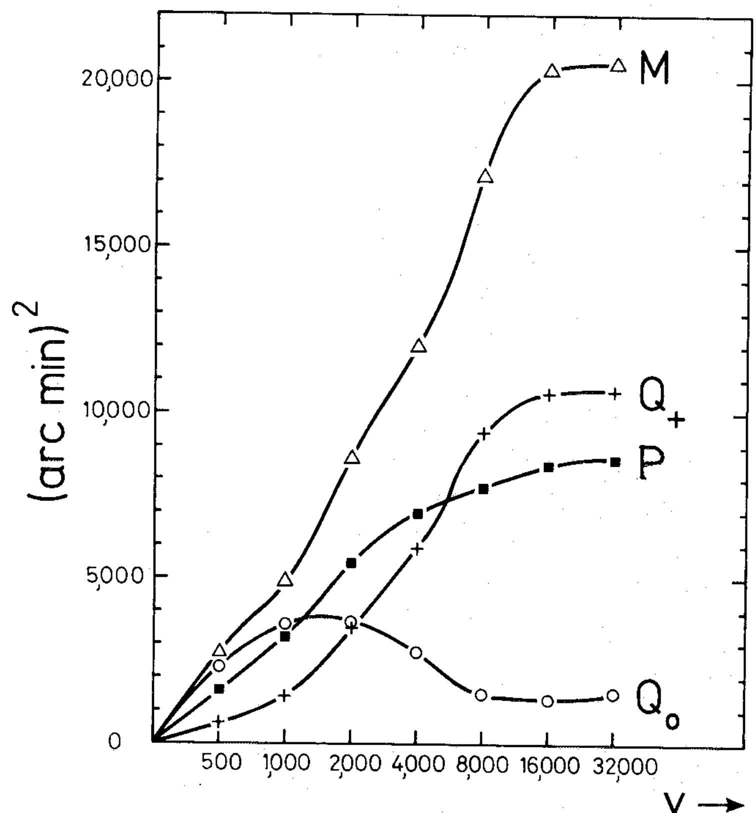

Figure 6. The growth of the magnitudes of the monopole, dipole and the quadrupole's positive eigenvalues as functions of the depth of sample – measured by Hubble velocity. All quantities are measured in arcmin^2. Notice the strength of Q_0 up to 1000 km s^{-1} and the saturation due to incompleteness beyond 12000. Q_- is the negative of the sum of Q_0 and Q_+.

With the negative eigenvector so close to the supergalactic pole the other two inevitably lie close to the supergalactic plane. Q_+ seems mainly influenced by the 'Great Attractor' and Perseus-Pisces directions (see Fig. 5). Two-thirds of Q_+ arises beyond 2000 km s^{-1} and almost a half beyond 4000 km s^{-1}. For large v this eigenvector points straight at the concentration in northern Centaurus that we identified with the Great Attractor, $l=308$, $b=27$. Of course quadrupole eigenvectors are equally associated with the opposite directions and $l=128$, $b=-27$ is not far from the Perseus-Pisces chain. To find out the main components of the brightness of the extragalactic sky, we have plotted the sky in equal area projections in supergalactic coordinates. Fig. 7(a) is centred on the northern supergalactic pole. The circle is the supergalactic equator, the grey scale is chosen so that black is more than twice the average density and white is less than half the average. The remarkable ring feature is the supergalactic band of bright galaxies.

The southern supergalactic hemisphere is poorly represented on this plot, as it is badly distorted by the projection with the southern supergalactic pole stretched into a circle around the whole. To see that hemisphere more compactly, we make the same projection centred on that southern pole and show it as Fig. 7(b). The net dipole's direction is the white cross. In Fig. 7(c,d) and (e,f) we show similar projections of the extragalactic sky brightness, but divide it into contributions with $v<2000$ km s^{-1} and with $v \geq 2000$ km s^{-1}, respectively. This allows us to distinguish contributions from the Virgo Supercluster from those from larger aggregates at greater distances. The Centaurus and Perseus regions are dominant in the $v \geq 2000$ km s^{-1} figures.

It is interesting to consider the shape of the 'light' ellipsoid, the squares of whose principal axes are $(\hat{\mathbf{r}}\cdot\mathbf{e}_1)^2$, $(\hat{\mathbf{r}}\cdot\mathbf{e}_2)^2$, $(\hat{\mathbf{r}}\cdot\mathbf{e}_3)^2$ weighted with the surface brightness of the sky ($\mathbf{e}_1$, $\mathbf{e}_2$, $\mathbf{e}_3$ are the unit eigenvectors of the quadrupole). These quantities are $M/3+(2/15)Q_+$, $M/3+(2/15)Q_0$ and $M/3+(2/15)Q_-$. We evaluate these for the well-determined range $v \leq 8000$ km s^{-1}. The square roots of these quantities are in the ratios 8:7:6 which therefore give the shape of the light ellipsoid generated by those galaxies. Whether the quadrupole continues to grow beyond 8000 km s^{-1} is not settled by the data of these catalogs. The monopole is believed to saturate in going to ∞ due to both finite age and redshift. The value obtained is some four times greater, which suggests final ratios of 29:28:27 for the total light ellipsoid if the quadrupole fails to grow any further. Such values show far greater anisotropy than the Cosmic Microwave Background.

The local gravity field is determined by the dipole, not the quadrupole. The latter tells us about regions in the sky from which excess gravity arises only to be cancelled by excess gravity from the opposite side of the sky – the dipole is the bit left over that indicates what area wins the tug-of-war. If we were to move away from the Local Group towards Centaurus, its influence would increase, whereas that of Perseus would decrease. Notice that the quadrupole Q^+ is surprisingly strong, larger than the dipole at large distances. The units are the same, Q^+ and **P** give the actual excess surface brightness due to those components in the eigenvector and dipole directions, respectively.

If we were to move away from the Local Group towards Centaurus its influence would increase whereas that of Perseus would decrease. If we moved half way to the Centaurus source of the quadrupole we might expect its gravity field to increase by a factor ~4 while that on the opposite side to change by a factor of $\frac{4}{9}$ assuming they were at equal distance. The actual effect will be smaller as the quadrupole is distributed and some of its sources will move on to the other side. The above calculation illustrates that the quadrupole is giving us information on how the gravity field changes as we change our viewpoint. The *Local gradient* of the gravity field strictly speaking needs the inverse-distance-weighted brightness quadrupole, *not* the brightness quadrupole we have calculated here. Raychaudhury & Lynden-Bell (1989) have calculated the former which converges more rapidly. The eigenvectors of our quadrupole in the $v<500$ km s^{-1} sphere agree well with theirs. Fig. 7(b) contrasts nicely with Fig. 7(a) to illustrate that a significant contributor to the dipole is the Hydra-Centaurus supercluster, but this impression has been considerably enhanced by the use of the Mock Sky. However, considerable contributions come from galaxies at lower velocities in those directions such as Cen A. Half the dipole arises below 2000 km s^{-1} and here Fig. 7(c,d) carry more information. Tully's Local Void occupies the central region of 7(e) including the northern supergalactic pole. The corresponding region in the supergalactic south is not so sparsely populated with galaxies in Fornax and Hydra, both contributing. The push from the Local Void, coupled with the pull from Virgo and Ursa Major, combine to give the local contribution to the dipole. Further analysis of the depth dependence of the dipole can be made using Table 3 which gives the x, y, z components of $\mathbf{P}(<v)$ and the $|P|$, l, b translations of them. The second half of the table gives $\mathbf{D}(v)=\mathbf{P}-\mathbf{P}(<v)$, which represents the gravitational force on a homogeneous sphere of 'radius' v, centred on the Local Group due to material outside that sphere. The main changes with redshift are the progressive weakening of $|D|$ accompanied by a progressive shift in its direction to lower galactic latitude as the effect of Virgo decreases in favour of Pavo-Indus-Telescopium.

It is now possible to provide some synthesis of this work and recent work on streaming motions. Whereas the Local Group's motion is governed by the gravity field *here*, the streaming motions are an average of gravity fields over quite a wide region. The Local gravity field is accurately aligned along the direction of motion of the Local Group. As we move away from the Local Group towards Perseus, that motion is opposed by the growing effect of the quadrupolar terms, but as we move away toward Centaurus, these terms enhance the dipole and swing it towards Centaurus. A third of it arises nearer than 1500 km s^{-1}, a further third

Table 3.

v	P_x / $\|P\|$	P_y / ℓ	P_z / b	D_x / $\|D\|$	D_y / ℓ	D_z / b
500	313	-1014	1216	346	-6575	2523
	1614	287	49	7050	273	21
1000	-91	-1901	2532	750	-5688	1207
	3168	267	53	5863	278	12
2000	29	-4048	3652	630	-3541	87
	5152	270	42	3598	281	1
4000	478	-5391	4408	274	-2097	-1038
	6981	275	39	2356	277	-26
8000	281	-6440	4255	371	-1149	-516
	7724	273	33	1313	278	-23
Total	659	-7589	3739	0	0	0
	8486	275	26	0	-	-

arises from Hydra-Centaurus and less than 25 per cent arises from the Centaurus Concentration at 4300 km s^{-1}. However, only a quarter of the Quadrupolar term arises in Hydra-Centaurus velocity range 2000–4000 km s^{-1}. About half of Q_+ arises from beyond that. At the Centaurus clusters the net gravity field will be dominated by those more distant sources, the major one of which will be the Centaurus Concentration. A spherically symmetric Great Attractor model centred on $v=4300$ km s^{-1} gives incorrect predictions. However, a more elongated Great Attractor caused by the large-scale density enhancement encompassing the Centaurus Concentration, Hydra-Centaurus and connected on to Telescopium- Pavo-Indus is consistent with the pictures of the sky given in Lynden-Bell *et al.* 1988 and the more recent redshift distributions found by Dressler 1988 and by Fairall 1988. This picture accords well with the picture of clusters of galaxies in chain-like configurations with the neighbouring agglomerations in the chain being the major influence on each in turn.

Galaxies over a wide region of the sky, stretching from $l=260$–340, $b=-35$ to $+40$, with radial velocities in the range 2000–4000 km s^{-1} collectively pull on us; the Centaurus Concentration at 4300 km s^{-1} is the major influence on the motions of those galaxies but only a minor contributor to the Local Group's motion.

Acknowledgments

The hard work of cataloging under the inspiration of Holmberg, Huchra and Vorontsov-Velyaminov has been vital. In particular the catalogs of Nilson & Lauberts form the basis for this paper. We thank S. Faber for stimulating it and Angela Samuels who wrote programs to incorporate the velocities of Huchra's catalog into ESO and UGC. In the end this was overtaken by Burstein's organization of all these catalogs into direct access files with pointers in each to corresponding entries in the others. These files have been our data source.

References

Boldt, E., 1987. *Phys Repts,* **146,** 215.
Burstein, D. & Heiles, C., 1978. *Astrophys. J.,* **225,** 40.
Burstein, D. & Lebofsky, M. J., 1986. *Astrophys. J.,* **301,** 683.
Chincarini, G. & Rood, H. J., 1979. *Astrophys. J.,* **230,** 648.
Conklin, E. K., 1969. *Nature,* **222,** 971.
da Costa, L. N., Nunez, M. A., Pellegrini, P. S. & Willmer, C., 1986. *Astr. J.,* **91,** 6.
Davis, M. & Huchra, J., 1982. *Astrophys. J.,* **254,** 437.

Dickens, R. J., Currie, M. J. & Lucey, J. R., 1986. *Mon. Not. R. astr. Soc.*, **220**, 679.
Dressler, A., 1987. *Sci. Am.*, **225**, 46.
Dressler, A., 1988. *Astrophys. J.*, **329**, 519.
Faber, S. M. & Burstein, D., 1988. In: *Large Scale Motions in the Universe, Proceedings of the Vatican Study Week*, eds Coyne, G. & Rubin, V. C., Princeton University Press, Princeton.
Fairall, A. P., 1988. *Mon. Not. R. astr. Soc.*, **230**, 69.
Fisher, J. R. & Tully, R. B., 1981. *Astrophys. J. Suppl.*, **47**, 139.
Fouqué, P. & Paturel, G., 1985. *Astr. Astrophys.*, **150**, 192.
Gunn, J. E., 1987. *Dark Matter in the Universe, IAU Symp. No. 117*, p. 542, eds J. Kormendy, J. & Knapp, G. R., Reidel, Dordrecht.
Harmon, R. T., Lahav, O. & Meurs, E. J. A., 1987. *Mon. Not. R. astr. Soc.*, **228**, 5P.
Henry, P. S., 1971. *Nature*, **231**, 518.
Hopp, U. & Materne, J., 1985. *Astr. Astrophys. Suppl.*, **61**, 93.
Huchra, J. P., 1989. *The Extragalactic Distance Scale*, A.S.P. Meeting, Victoria, 1988.
Kaiser, N. & Lahav, O., 1988. In: *Large Scale Motions in the Universe, Proceedings of the Vatican Study Week*, p. 339, eds Coyne, G. & Rubin, V. C., Princeton University Press, Princeton.
Lahav, O., 1987. *Mon. Not. R. astr. Soc.*, **225**, 213.
Lahav, O., Rowan-Robinson, M. & Lynden-Bell, D., 1988. *Mon. Not. R. astr. Soc.*, **234**, 677.
Lahav, O., Edge, A. C., Fabian, A. C. & Putney, A., 1989. *Mon. Not. R. astr. Soc.*, in press.
Lauberts, A., 1982. *The ESO-Uppsala Survey of the ESO(B) Atlas*, European Southern Observatory.
Lubin, P. & Villela, T., 1986. In: *Galaxy Distances and Deviations from Universal Expansion*, p. 169, eds Madore, B. F. & Tully, R. B., Reidel, Dordrecht.
Lucey, J. R., Currie, M. J. & Dickens, R. J., 1986. *Mon. Not. R. astr. Soc.*, **221**, 467.
Lynden-Bell, D., 1986. *Q. Jl R. astr. Soc.*, **27**, 319.
Lynden-Bell, D., 1987. *Jl R. astr. Soc.*, **28**, 186.
Lynden-Bell, D. & Lahav, O., 1988. In: *Large Scale Motions in the Universe, Proceedings of the Vatican Study Week*, p. 199, eds Coyne, G. and Rubin, V. C., Princeton University Press, Princeton.
Lynden-Bell, D., Faber, S. M., Burstein, D., Davies, R. L., Dressler, A., Terlevich, R. J. & Wegner, G., 1988. *Astrophys. J.*, **326**, 19.
Meiksin, A. & Davis, M., 1986. *Astr. J.*, **91**, 191.
Melnick, J. & Moles, M., 1987. *Rev. Mex. Astr. Astrophys.*, **14**, 72.
Nilson, P., 1973. *Uppsala General Catalogue of Galaxies, Uppsala astr. Obs. Ann.*, **6**.
Paturel, G., Bottinelli, L., Gougenheim, L. & Fouqué, P., 1988. *Astr. Astrophys.*, **189**, 1.
Peebles, P. J. E., 1980. *The Large Scale Structure of The Universe*, Princeton University Press, Princeton.
Plionis, M., 1988. *Mon. Not. R. astr. Soc.*, **234**, 401.
Raychaudhury, S. & Lynden-Bell, D., 1989. *Mon. Not. R. astr. Soc.*, in press.
Richter, O. G., 1984. *Astr. Astrophys. Suppl.*, **58**, 131.
Scaramella, R., Baiesi-Pillastrini, G., Chincarini, G., Vettolani, G. & Zamorani, G., 1988. *Nature*, **338**, 562.
Shafer, R. A. & Fabian, A. C., 1983. In: *Early Evolution of the Universe and Its Present Structure, IAU Symp. No. 104*, eds Abell, G. O. & Chincarini, G., Reidel, Dordrecht.
Shaya, E. J., 1984. *Astrophys. J.*, **280**, 470.
Strauss, M. A. & Davis, M., 1988. In: *Large Scale Motions in the Universe, Proceedings of the Vatican Study Week*, p. 256, eds Coyne, G. & Rubin, V. C., Princeton University Press, Princeton.
Strukov, I. A., Skulachev, D. P., Boyarskii, M. N. & Tkachev, A. N., 1987. *Soviet Astr. Lett.*, **13**, 65.
Tammann, G. & Sandage, A., 1985. *Astrophys. J.*, **294**, 81.
Villumsen, J. V. & Strauss, M. A., 1987. *Astrophys. J.*, **322**, 37.
Vorontsov-Velyaminov, B. A. & Arkipova, A. A., 1963–68. *Morphological Catalogue of Galaxies*, Moscow State University, Moscow.
Yahil, A., 1988. In: *Large Scale Motions in the Universe, Proceedings of the Vatican Study Week*, p. 219, eds Coyne, G. & Rubin, V. C., Princeton University Press, Princeton.
Yahil, A., Sandage, A. & Tammann, G. A., 1980. *Astrophys. J.*, **242**, 448.
Yahil, A., Walker, D. & Rowan-Robinson, M., 1986. *Astrophys. J.*, **301**, L1.

Appendix A: Nomenclature and history of terms

There is continuing confusion over the terminology related to the Centaurus direction for the following reasons: several distinct clumps of galaxies exist at different distances in the direction of the Centaurus constellation; the redshift distance is not the true distance and, finally, the

Table A1. Regional terminology related to large-scale motions.

Name Source	Location (Gal.Coord.) and/or Angular Extent	Range of Radial Velocity
Hydra-Centaurus (Chincarini & Rood 1979)	$\ell = 285$,b=25	2000-4300 km/s
Centaurus Cluster (Dickens *et al.* 1986;	$\ell = 302$,b=21 circle 6° radius	2000-5000 km/s
Centaurus Concentration (Lynden-Bell *et al.* 1988; da Costa *et al.* 1986)	$\ell = 310$,b=29 ellipse 15° × 30° along supergalactic equator	4300± 1000 km/s
Pavo-Indus-Telescopium (Dressler 1988; Fairall 1988)	$\ell = 320 - 360$, b=−35 to 0	3000-6000 km/s
'Great Attractor Region' Dressler 1988)	$\ell = 290 - 350$, b=−35 to 45	2000-6000 km/s
'Great Attractor Model'		
Lynden-Bell *et al.* 1988;	centred at $\ell = 307$,b=9	distance 4300 ± 500
Faber & Burstein 1988	centred at $\ell = 309$,b=18 core of 1500 km/s	distance 4200 ± 300

distribution of matter can be predicted either from the velocity field or from the galaxy distribution.

We summarize our understanding of the relevant terms in Table A1. Chincarini & Rood (1979) recognized Hydra-Centaurus as a possible nearby supercluster. Shaya (1984) and Tammann & Sandage (1985) suggested that Hydra-Centaurus, along with Virgo, were responsible for the Local Group's motion. As used in this paper, the term Centaurus Concentration will refer to the apparent feature centred at $l = 310$, $b = 29$, that has a mean heliocentric velocity of 4300 km s^{-1} (fig. 8 of Lynden-Bell *et al.* 1988, da Costa *et al.* 1986; see also Dressler 1988), with a standard deviation in the velocities of individual galaxies of 1000 km s^{-1}. This concentration is flattened along the supergalactic plane. It includes the clusters Klemola 27 = IC 4329 cluster (see Richter 1984) and IC 4296. It does not include the Cen 30, Cen 45 cluster(s) in Southern Centaurus (below). All the above clusters have been considered part of the Hydra Centaurus supercluster that extends over to the Antlia cluster (Hopp & Materne 1985).

The Centaurus Clusters will refer to the clusters studied by Dickens, Currie & Lucey (1986), denoted as Cen30 and Cen45 by them, and labelled by a 'C' in fig. 8 of Lynden-Bell *et al.* (1988). The relationship of the clusters to field galaxies in the Hydra-Centaurus region is discussed by Lucey *et al.* (1986). Laubert's map (1982) shows the great swathes of galaxies across the southern sky. Lahav's plots of UGC and ESO show apparent connections to Northern features described in Lynden-Bell (1986). Faber, Lynden-Bell & Lahav (in Lynden-Bell 1987) drew attention to the remarkable structure centred near the Centaurus Concentration and stretching across the sky from Virgo across the galactic plane to Pavo-Indus-Telescopium. Paturel *et al.* (1988) found the same feature in their galaxy charts and called it a Milky Way of galaxies.

The term Great Attractor was invented by Alan Dressler for an agglomeration of matter that caused the galaxy streaming. The term has been used in two ways: (i) for the spherically symmetric Great Attractor models of Lynden-Bell *et al.* (1988) and Faber & Burstein (1988) which put the centre of attraction at a distance of 4000–4500 km s^{-1} and attribute much of the Local Group's motion to it. These models conflict with the findings reported here. (ii) Dressler

(1988) and Fairall (1988) found that Pavo-Indus-Telescopium on the other side of the Milky Way connect continuously in redshift to the Centaurus region as they appear to do in Laubert's map. Dressler (1988) (see also 1987) used the term Great Attractor for a region of enhanced density subtending about a steradian in the sky in which the Centaurus Concentration, the Centaurus clusters and Pavo-Indus-Telescopium are also included.

Another strong and broad clump lies in the Centaurus direction but much further away at 14 000 km s^{-1}, centred on Shapley 8. The clump is seen in the distribution of galaxies (Melnick & Moles 1987), Abell-Corwin clusters (Scaramella *et al.* 1988) and X-ray clusters (Lahav *et al.* 1989).

Appendix B: Evaluation of $\bar{D}$

$$\bar{D} = -\int_0^\infty D\, d\mathscr{L}/dD\, dD = -D_{\rm L}\int_0^\infty t^{1/2} d\mathscr{L}/dt\, dt$$

$$= D_{\rm L}(\tfrac{1}{2} - 1/\beta)a^\beta \int_0^\infty t^{1/2}(1+t)(a+t)^{-\beta} dt$$

with $a=\beta=5$. Define

$$I(a) = \int_0^\infty t^{1/2}(1+t)(a+t)^{-3} dt.$$

Then

$$\bar{D} = D_{\rm L}(\tfrac{1}{2} - 1/\beta)a^\beta I''(a)/12$$

putting $t = a\tan^2\phi$ we find

$$I(a) = \int_0^{\pi/2} 2a^{-3/2}\sin^2\phi(\cos^2\phi + a\sin^2\phi)\, d\phi$$

$$I(a) = \left(\frac{\pi}{8}\right) a^{-3/2}(3a+1).$$

Hence for $a=5$

$$a^5 I''(a)/12 = \frac{\pi}{32}5^{5/2}$$

and

$$\bar{D} = D_{\rm L} 3\pi 5^{3/2}/64 = 1.65 D_{\rm L}.$$